



Hydrogen Decrepitation Press-Less Process Recycling of NdFeB sintered magnets

Xia, Manlong; Abrahamsen, Asger Bech; Bahl, Christian; Veluri, Badrinath ; Søgaard, Allan I. ; Bøjsøe, Poul

Published in:
Journal of Magnetism and Magnetic Materials

Link to article, DOI:
[10.1016/j.jmmm.2017.01.049](https://doi.org/10.1016/j.jmmm.2017.01.049)

Publication date:
2017

Document Version
Peer reviewed version

[Link back to DTU Orbit](#)

Citation (APA):
Xia, M., Abrahamsen, A. B., Bahl, C., Veluri, B., Søgaard, A. I., & Bøjsøe, P. (2017). Hydrogen Decrepitation Press-Less Process Recycling of NdFeB sintered magnets. *Journal of Magnetism and Magnetic Materials*, 441, 55-61. <https://doi.org/10.1016/j.jmmm.2017.01.049>

General rights

Copyright and moral rights for the publications made accessible in the public portal are retained by the authors and/or other copyright owners and it is a condition of accessing publications that users recognise and abide by the legal requirements associated with these rights.

- Users may download and print one copy of any publication from the public portal for the purpose of private study or research.
- You may not further distribute the material or use it for any profit-making activity or commercial gain
- You may freely distribute the URL identifying the publication in the public portal

If you believe that this document breaches copyright please contact us providing details, and we will remove access to the work immediately and investigate your claim.

Hydrogen Decrepitation Press-Less Process Recycling of NdFeB sintered magnets

Manlong Xia^{1,a}, Asger B. Abrahamsen^{2,b}, Christian R. H. Bahl¹, Badrinath Veluri³, Allan I. Sørensen⁴ and Poul Bøjsøe⁵

¹Department of Energy Conversion and Storage, Technical University of Denmark, DK-4000 Roskilde, Denmark

²Department of Wind Energy, Technical University of Denmark, DK-4000 Roskilde, Denmark

³GRUNDFOS A/S, DK-8850 Bjerringbro, Denmark

⁴Sintex A/S, DK-9500 Hobro, Denmark

⁵Holm Magnetic Aps, DK-2800 Kgs Lyngby, Denmark

Corresponding Author: Asger B. Abrahamsen, asab@dtu.dk

Abstract

A Hydrogen Decrepitation Press-Less Process (HD-PLP) recycling method for recycling of anisotropic NdFeB magnets is demonstrated. The method combines hydrogen decrepitation (HD) disintegration of the initial magnet, powder sieving and the Press-Less Process (PLP), where hydride powder is sintered in a graphite mold. Coercivities up to 534 kA/m were obtained in porous samples based on powder size $d < 100 \mu\text{m}$. Adding a ball milling step resulted in full density isotropic magnets for $d > 100 \mu\text{m}$. The coercivity reached $H_{ci} = 957 \text{ kA/m}$ being 86 % of the original N48M material without addition of rare earth elements.

Highlights:

- 1) Demonstration of a Hydrogen Decrepitation Press-Less Process (HD-PLP) recycling method of sintered NdFeB permanent magnets.
- 2) Direct recycling of NdFeB magnets without any addition of material.
- 3) Magnetic phase diagram determined of recycled magnets produced from both hydride and ball milled powder.

Keywords: Recycling, NdFeB sintered magnet, Press-Less Process

Abbreviations

PLP Press-Less Process

HD Hydrogen decrepitation

HDDR Hydrogenation Disproportionation Desorption and Recombination

NdFeB	Neodymium Iron Boron permanent magnets
VSM	Vibrating Sample magnetometer
SEM	Scanning Electron Microscopy
ICP	Inductively Coupled Plasma spectroscopy

Acknowledgement

The authors would like to acknowledge Dr. Didier Blanchard and Dr. Yunzhong Chen at the Department of Energy Conversion and Storage for assistance on the hydrogenation processing and VSM measurements respectively. This work is part of the REEgain project supported by the Innovation Fund Denmark.

1 Introduction

The Nd₂Fe₁₄B (NdFeB) ferromagnetic alloy discovered in 1983 by Sagawa plays an important role in industrial applications due to its superior magnetic properties[1]. NdFeB magnets are used in a wide range of clean energy and high tech applications, such as wind turbines, electric vehicles and computers[2]. A large effort has been focused on how to guarantee the supply and to reduce the usage of heavy rare earth elements in NdFeB permanent magnets for these applications. With life times of wind turbines of 20-25 years it is expected that large amounts of NdFeB magnets for recycling will become available as permanent magnet direct drive turbines are decommissioned[2]. Thus it is believed that recycling will be increasingly important for the transition of the energy sector towards more renewable sources. There are mainly two methods to recycle NdFeB sintered magnets into new magnets. One is to mill hydrogenated NdFeB powder, aligning, compacting by pressing and finally vacuum sintering[3]. The other is to use the Hydrogenation Disproportionation Desorption and Recombination (HDDR) process to produce anisotropic or isotropic powder, which can be used to produce polymer bonded magnets[4]. The first method can provide high magnetic properties but the cost is almost the same as that of the original magnet. In contrast, the HDDR process may be cheaper, but provides lower magnetic properties.

In this paper it is investigated if the Press-Less Process (PLP) [5,6] can be used to recycle sintered NdFeB magnets. The press-less process was developed to improve the coercivity of NdFeB sintered magnets by decreasing the particle size of the initial magnet alloy powder to below 2 μm in order to obtain a higher density of grain boundaries to prevent the movement of the magnetic domain walls [7]. This allowed the removal of dysprosium from PLP magnets for high temperature applications and thereby lifted the dependency of the heavy rare earths [7]. The challenge of using small particles in conventional NdFeB magnet manufacturing is that the powder will tend to get stuck in the pressing die. The press-less process is therefore based on sintering the fine magnetic alloy powder in a graphite mold after a packing of the initial powder to about half of the bulk density of the magnet [6].

The main motivation for using the press-less process for sintering of recycled magnets is that if the initial material is an anisotropic magnet, hydrogen can be used to break up the magnet into smaller particles, that by nature all will be anisotropic, and therefore be possible to align and sinter even if they are about 10 times larger than what is usually used for the press-less process. Secondly, it is expected that the cost of the Hydrogen Decrepitation Press-Less Process (HD-PLP) recycling might be lower than for the original press-less process used with small particle powder, because the demand for high purity gasses for jet-milling and handling atmosphere in the glovebox seems lower due to lower oxidation of the large particles. Compared to the more traditional method based on pressing of the green sample before sintering [8], one can omit a pressing machine, which will also contribute to a cost reduction.

2 Experimental method

Fig.1 shows a schematic description of the recycling process applied. Passivated commercial N48M magnets were used as initial material for the recycling process in order to represent magnets obtained from an end of life product. The magnetic properties of the original N48M magnets are a coercivity of $H_{ci} = 1114$ kA/m, a remanence of $B_r = 1.39$ T and a maximum energy product of $(BH)_{max} = 370$ kJ/m³. The composition of the magnets are approximately Nd_{10.7}Pr_{2.68}Dy_{0.43}Fe_{79.2}B_{5.75}Co_{0.79}Al_{0.19}Cu_{0.11} (atomic fraction in %) as determined by inductively coupled plasma (ICP) spectroscopy. The microstructure of the initial magnet shown in figure 2 was obtained by Scanning Electron Microscopy (SEM). The N48M magnets were subjected to $P_{H_2} = 4.5$ bar of hydrogen for 2 hours at room temperature in a sealed container, whereby the magnets were disintegrated into powder as shown in fig 1. A typical hydrogen pressure drop in the order of $\Delta P_{H_2} = 0.8$ bar indicates that hydrogen was incorporated into the magnet alloy and changed the composition to R₂Fe₁₄BH_x, where $x \sim 3.5$.

The hydride powder resulting from the disintegration of the N48M magnets was subsequently handled in an argon glovebox in order to avoid oxidation. The HD process resulted in a large fraction of powder with a particle size larger than 100 μ m, which is too large to result in a successful sintering. Using a 100 μ m, 50 μ m and 28 μ m sieve the different particle size fractions were separated (Fig 1). The size fractions were filled into $D_{inner} = 7$ mm and $L = 14$ mm cylindrical graphite crucibles and packed by pressing a rod into the crucible to obtain a resulting apparent powder density of $\rho_{powder} = 3$ g/cm³, which is less than half the density of the original magnet $\rho_{N48M} = 7.56$ g/cm³. These samples are termed '*hydride sample*'.

In order to improve the amount of powder with a size fraction lower than 100 μ m a ball milling step was introduced before the sieving of the powder. The ball milling was done by placing 202 g of hydride powder in a 250 ml ball milling container together with steel balls (188 g Ø10mm, 128 g Ø5mm and 88 g Ø3mm) in argon. The total weight of the balls was 404 g and resulted in a ball to powder weight ratio of 2:1. The powder was milled under argon for 3 hours at 650 rpm in a Fritch P6 ball mill. The samples prepared from the ball milled powder are termed '*ball milled*'.

Some of the samples were aligned with a $B_a = 1.5$ T slowly ramped magnetic field applied either parallel or perpendicular to the crucible cylinder direction (Fig 1). This was done outside the glovebox, while keeping the samples in an argon filled plastic bag. Samples with powder aligned by

an external magnetic field are termed anisotropic, whereas non-aligned samples are termed isotropic. All samples were transported into a vacuum furnace connected to the glovebox and sintered at $T_{\text{sinter}} = 1110$ °C for 2 hours after first evacuating the furnace to 10^{-4} mbar using a turbo pump.

Degassing temperature ramps of 2 °C/min (room temperature to 250 °C and 1 hour hold), 2 °C/min (250 to 570 °C and 1 hour hold) and 5 °C/min (570 to T_{sinter}) were used and a cooling rate of 25 °C/min was used after the sintering hold time. The samples were removed from the graphite crucibles by turning them upside down, whereby they fell out since the samples were shrinking during the sintering (Fig 1). Smaller pieces for characterization of the samples were cut using a diamond saw.

The magnetic properties of the samples with a typical size of 1 mm³ were characterized using a high temperature option of a vibrating sample magnetometer (VSM) from Cryogenic limited. The microstructure was investigated by Scanning Electron Microscopy (SEM) using a TM3000 from Hitachi after epoxy casting and polishing of the samples.

3 Theory and calculations

Normalization of the magnetization measurements was done using the sample mass m_s and the sample volume V , whereby the volume magnetization density becomes

$$M = \frac{m}{V} = \frac{m\rho_s}{m_s} = M_{\text{int}} \frac{\rho_s}{\rho_{\text{ideal}}} \quad (1)$$

where m is the magnetic moment and ρ_s is the mass density of the sample. In order to compare samples with different densities then the intrinsic properties were obtained by assuming an ideal density of $\rho_{\text{ideal}} = 7.5$ g/cm³, whereby

$$M_{\text{int}} = \frac{m\rho_{\text{ideal}}}{m_s} \quad (2)$$

is the intrinsic volume magnetization density as if the sample had full density.

Correction for the demagnetization field was made and the resulting internal field was found as

$$H = H_a - NM \quad (3)$$

where H_a is the applied field, N the demagnetization factor based on the sample dimensions [9] and M the volume magnetization density. In the following figures the intrinsic magnetization density M_{int} is shown as function of the internal field H .

4 Results

The sample dimensions shrink during the sintering and the densities were in the range $\rho_{\text{Hydride}} = 3.7$ - 6.9 g/cm³ for the hydride samples and $\rho_{\text{Ballmill}} = 7.1$ - 7.4 g/cm³ for the ball milled samples respectively as listed in Table 1.

Fig. 3a-c show the microstructure of the magnets obtained from $d = 50\text{-}100\ \mu\text{m}$, $d = 28\text{-}50\ \mu\text{m}$ and $d < 28\ \mu\text{m}$ hydride powder. It is observed that pores are present and that the pore density is decreasing with a smaller particle powder fractions size. The densities of the samples are increasing from 4.6, 5.8 and finally 6.9 g/cm³ for the 50-100 μm , 28-50 μm and $d < 28\ \mu\text{m}$ size fractions respectively. Thus almost full density samples are only obtained for the smallest size fraction resulting in a rather low yield of the process. Fig. 4a and b show the microstructure of isotropic ball milled magnets made from $d = 50\text{-}100\ \mu\text{m}$ and $d = 28\text{-}50\ \mu\text{m}$ powder. The yield of powder with $d < 28\ \mu\text{m}$ was very small, because the powder was sticking to the balls and wall of the ball milling container. The images reveal a quite low and similar pore concentration, which is comparable to what is observed for the hydride $d < 28\ \mu\text{m}$ magnet shown in fig 3c. The low pore concentration is also reflected in densities of the samples based on the ball milled powder being in the range of 7.1 - 7.4 g/cm³.

Fig. 5 shows the intrinsic magnetic properties of selected hydride and ball milled samples as well as the original N48M magnet at room temperature $T = 20\ ^\circ\text{C}$. It should be noted that the magnetization curves of the hydride and ball milled samples are isotropic and are shown as the intrinsic properties as if no pores were present in the sample using the method outlined in section 3. The magnetization curve of the original N48M anisotropic magnets with the applied field along the easy axis is also shown for comparison.

The magnetic properties of the dry ball milled and the hydride samples of fig. 5 are summarized in table 1 along with the densities of the samples. Fig. 6 is showing the magnetization curve of aligned samples based on hydride powder smaller than 100 μm obtained by sieving. The intrinsic magnet properties are included in table 1.

The temperature dependences of the intrinsic remanence and the coercivity of both the isotropic and anisotropic recycled samples and the original anisotropic magnet are shown in Fig. 7. With an increasing temperature, the coercivity and remanence of all the samples decrease as the Curie temperature is approached. When these samples are cooled down to room temperature again, some samples recover their initial room temperature properties. However, that is not always the case for the hydride powder samples and the temperature history is indicated with arrows in Fig. 7. It is observed that the 28-50 μm and 50-100 μm hydride powders do not recover after heating to 160 $^\circ\text{C}$ in the vacuum of the VSM sample chamber. However, the sample with a particle size smaller than 28 μm did recover its original properties. All the ball milled samples recovered their initial properties after returning to room temperature.

5 Discussion

The mass densities of the HD-PLP samples after sintering are indicating that the hydride powder results in more pores than the ball milled powder, which is confirmed by the SEM images in fig 3 and 4. The pore size seems to be related to the sieve mesh size in case of the hydride powder, but not for the ball milled powder. This is probably, because the ball milling of the powder results in agglomeration of particles smaller than 28 μm as no powder size fraction of $d < 28\ \mu\text{m}$ was obtained by sieving. Thus, the sieving of the ball milled powder provides the size fractions of agglomerates, which consist of much smaller particles. In previous experiments, the agglomerations stuck to the wall of the container after ball milling strip cast material were examined by dissolving and agitating the agglomerates in ethanol and using a laser diffraction method to determine the size distribution. Those studies indicated that the mean particle size of the agglomerates was in the order

10 μm . Thus, it seems likely that the sieved agglomerates of the ball milled hydrides in the present series consist of such small particles in the order of 10 μm and they therefore sinter into a similar final structure as seen on fig 4. In order to compare the internal properties of the different samples the method of calculating the intrinsic magnetic properties were introduced in section 3. The idea is to compare the volume magnetization density of the material as if there were no pores in order to identify the potential of the recycled magnets. The magnetization curves of fig 5 are showing that the hydride samples have coercivities in the range 300-500 kA/m at room temperature, whereas the samples based on ball milled powder are reaching 950 kA/m. The latter values are approaching the properties of the original magnet having a coercivity of 1114 kA/m and shows that the HD-PLP recycling method is working without any addition of new material or rare earth elements. The remanence B_r shown in figure 5 is the intrinsic remanence of isotropic samples and this is compared to the anisotropic initial magnet. A simple way to compare an anisotropic to an isotropic sample is to assume that domains of the fully aligned original anisotropic sample preserve their magnetization density M_0 and are put together with random orientation. The measured magnetic moment M_{iso} will then only be the component $M_0 \sin(\theta)$ projected onto the applied magnetic field direction along the symmetry axis of the pickup coils of the VSM. The density of particles with an orientation angle θ with respect to the coil plane is scaling as $\cos(\theta)$, whereby

$$M_{iso} = \int_0^{\pi/2} (M_0 \sin(\theta) \cos(\theta)) d\theta = \frac{M_0}{2} \quad (4)$$

where an integration over the domain orientations is done[10]. From table 1 it is seen that the ratio between the remanence of the HD-PLP samples and the original sample is $B_r/B_0 \sim 0.5$, which is indicating a full recovery of the magnetic moment of the original sample according to eq. (4).

The anisotropic samples obtained from the hydride powder with $d < 100 \mu\text{m}$ have coercivities in the range 490-530 kA/m, which is comparable to the other hydride powder with $d = 28-50 \mu\text{m}$, but not the $d = 50-100 \mu\text{m}$. This might be due to a larger fraction of the $d = 28-50 \mu\text{m}$ size is present in the $d < 100 \mu\text{m}$ powder. The intrinsic remanence is seen to increase by the alignment field and the loose powder is easier to reorient than the powder, which is first compacted to an apparent density of 3 g/cm³. The remanence is approaching the values of the initial magnet and further studies have to reveal if a higher alignment field will result in a better alignment of the final samples. It is remarkable that the hydride powder with a size fraction that is much larger than the typical size $d = 1-20 \mu\text{m}$ of jet milled strip cast flake can be aligned by the external magnetic field. We believe this is possible, because the initial anisotropic sintered magnets consist of fully aligned material, which is broken up by the hydrogen decrepitation process into fractures holding many aligned grains of the initial structure. Introducing the hydrogen into the magnetic alloy removes the coercivity of the $\text{R}_2\text{Fe}_{14}\text{B}$ phase, but the magnetic easy axis of the $\text{R}_2\text{Fe}_{14}\text{BH}_x$ phase still results in a torque large enough to rotate the fractures. The alignment of the ball milled powder has not yet been examined, but it is expected that the agglomeration of the small particles might make the alignment more difficult if the agglomerates are oriented randomly and if they are mechanically welded together.

The sintering process is initiated with two degassing steps in order to release the hydrogen absorbed in the hydride powder. The first degassing step at $T = 250 \text{ }^\circ\text{C}$ for 1 hour in high vacuum of 10^{-4} mbar is believed to primarily start the hydrogen release from the $\text{R}_2\text{Fe}_{14}\text{BH}_x$ phase ($\text{R}_2\text{Fe}_{14}\text{BH}_x \rightarrow \text{R}_2\text{Fe}_{14}\text{B} + x/2 \text{ H}_2$) in the grains as well as a first release of some of rare earth element rich phases in between the gains ($\text{NdH}_{2.7} \rightarrow \text{NdH}_2 + 0.35\text{H}_2$) [11]. Secondly this step is also intended to remove absorbed gasses or water from the surface of the hydride powder in order to prevent reactions with

the powder at higher temperature. The second degassing step at $T = 570\text{ }^{\circ}\text{C}$ for 1 hour is intended to transform the rare earth element hydride phase back into the pure rare earth elements ($\text{NdH}_2 \rightarrow \text{Nd} + \text{H}_2$) [11]. The clear advantage of the HD-PLP recycling method is that the low apparent powder density of 3 g/cm^3 of the sample before the sintering is providing a porous structure with a gas percolation path between the particles. The hydrogen from the hydride powder is therefore released more easily than from the green compacts after pressing used in the traditional method for production of sintered magnets. It is believed that the sample contains fractures of the original magnet after heating to $T > 570\text{ }^{\circ}\text{C}$ and that these fractures are re-sintered at higher temperature by the rare earth rich phases, which are expected to have released all the hydrogen. Thus the densification of the samples is first expected to take place after the hydrogen release has taken place.

A remaining question is: What is determining the pore size in the magnets if the hydrogen is released before the sintering? This can be addressed by considering a simple packing of identical spheres as shown on fig. 8. If the structure is assumed as simple cubic (SC) packing (fig. 8a) then the volume fraction is

$$f_{vol,SC} = \frac{\frac{4}{3}\pi r^3}{a_1^3} = \frac{\pi}{6} \sim 0.52 \quad (5)$$

since the unit cell side $a_1 = 2r$. The apparent mass density of such a powder will be $\rho_{SC} \sim 0.52 \rho_{\text{NdH}_2} \sim 3.9\text{ g/cm}^3$ and is close to the initial packing density of the PLP method. The powder is densified during the sintering and this can be obtained by sliding every second plane of the simple cubic packing structure towards the center of the unit cell, whereby a body centered cubic (BCC) packing results as shown in Fig. 8b. The volume fraction of the BCC packing is

$$f_{vol,BCC} = \frac{2 \cdot \frac{4}{3}\pi r^3}{a_2^3} = \frac{\sqrt{3}\pi}{8} \sim 0.68 \quad (6)$$

since $a_2 = \frac{4}{\sqrt{3}}r$. Thus the apparent mass density of such a structure is expected to be $\rho_{BCC} \sim 0.68 \rho_{\text{NdH}_2} \sim 5.2\text{ g/cm}^3$. One can also estimate the pore sizes l_1 and l_2 for the BCC packing as illustrated on figure 8b

$$l_1 = a_2 - 2r = 2 \left(\sqrt{\frac{4}{3}} - 1 \right) r \sim 0.3 r \quad (7)$$

$$l_2 = \sqrt{2}a_2 - 2r = 2 \left(\sqrt{\frac{8}{3}} - 1 \right) r \sim 1.3 r \quad (8)$$

If it is assumed that the first part of the densification of the samples during the sintering is caused by a reorganization of the powder similar to the simple cubic to BCC transformation then an estimate of the order of magnitude of the pores size will be related to the diameter d of the particles by $l_{\text{pores}} \sim 0.15 - 0.6 d$ as indicated by eq. (7) and eq. (8). Looking at the SEM images of the samples based on the $d = 50 - 100\text{ }\mu\text{m}$ hydride powder one would expect $l_{\text{pores}} \sim 8 - 60\text{ }\mu\text{m}$, which is also what is observed. Secondly the expected apparent mass density of the sample should be around 5.2 g/cm^3 , which is close to the values listed in table 1. For the $d = 28 - 50\text{ }\mu\text{m}$ hydride powder one

would expect $l_{\text{pores}} \sim 4 - 30 \text{ } \mu\text{m}$, whereas for $d < 28 \text{ } \mu\text{m}$ the pores size is expected to be $l_{\text{pores}} < 4 - 17 \text{ } \mu\text{m}$. Thus for the smaller powder size fraction the pores are getting small enough to support the mass transport of the sintering process, whereby full density samples can be obtained. This analysis also support the observation that all the size fractions of the ball milled powder result in full density samples as shown in table 1, because the particles in the agglomerates have a size around $10 \text{ } \mu\text{m}$, whereby the $l_{\text{pores}} \sim 6 \text{ } \mu\text{m}$ as seen on the SEM images of fig. 4.

The final magnetic phase diagram of the HD-PLP magnets in figure 7 shows that the remanence is scaling with temperature as the original magnet for the samples that have full density, but not for some of the hydride samples, which show a decrease in the magnetic properties when cooled down to room temperature. This effect is believed to be caused by the presence of a low but significant concentration of oxygen in the VSM during the measurements. The VSM is constantly pumping on the sample volume in order to provide thermal insulation between the heated aluminum oxide sample stick, where the samples are mounted in an aluminum oxide cup, and the measuring coils of the VSM sitting in the variable temperature insert of the VSM setup. The pressure of the vacuum is estimated to be approximately 10 mbar, whereby the resulting back streaming of oxygen through the pump is estimated to be $p_{\text{O}_2} \sim 10^{-2} \cdot 21 \% \sim 2100 \text{ ppm}$. This is a relatively high concentration of oxygen, which can cause a degradation of the magnetic properties of samples if they are porous. The fact that the samples with an apparent density in the order of $4\text{-}5 \text{ g/cm}^3$ are showing degradation is seen as an indication that there is a gas percolation path between the particles whereby the oxygen can react with a large fraction of the sample compared to just a surface layer of the dense samples.

The origin of the coercivity in the samples is believed to be caused by the original microstructure of the starting N48M magnet material, where rare earth rich phases are separating the $\text{R}_2\text{Fe}_{14}\text{B}$ grains [12]. The introduction of the hydrogen will enter the rare earth rich phases and break up the original structure into fractures [13]. These fractures will loose their magnetic properties due to the hydrogen [11] and the release of this hydrogen during the degassing stages of the sintering might be a factor limiting how much of the initial coercivity that can be recovered. If this picture is correct one would expect an easier hydrogen release and thereby an increasing coercivity with a decreasing fracture size. Looking at table 1 it is seen that the large hydride fractures are resulting in the lowest coercivity and that the ball milled powder consisting of agglomerates of small particles result in the highest coercivity. Thus further work on the optimization of the temperature profile might result in better recovery of the coercivity.

6 Conclusion

It has been demonstrated that a new recycling method, which is combining Hydrogen Decrepiation of anisotropic sintered NdFeB magnets with the Press-Less Process, where powder is sintered in graphite crucibles can produce isotropic and anisotropic magnets without any addition of new material. The method is termed HD-PLP recycling due to the combination. Magnets have been produced directly from hydride powder, but do only become dense when the powder size is below $28 \text{ } \mu\text{m}$. Adding a ball milling step resulted in further disintegration of the hydride powder and dense samples could be produced. The coercivity of the samples reached $H_{\text{ci}} = 534 \text{ kA/m}$ and $H_{\text{ci}} = 957 \text{ kA/m}$ when based on the hydride powder and ball milled powder corresponding to 48 % and 86 % of the coercivity of the original N48M magnet.

Preparation	Alignment	Sieve fraction [μm]	B_r [T]	H_{ci} [kA/m]	Density [g/cm ³]
Hydride	Isotropic	< 28	0.51	297	6.9
		28-50	0.78	499	5.8
		50-100	0.72	304	4.6
Hydride and ball milled	Isotropic	28-50	0.69	957	7.4
		50-100	0.69	955	7.1
		> 100	0.69	870	7.3
Hydride Tapped	Anisotropic $B \perp$ crucible	< 100	0.92	519	4.9
	Anisotropic $B \parallel$ crucible	< 100	1.01	493	5.3
Hydride Loose	Anisotropic $B \perp$ crucible	< 100	1.19	534	3.7
N48M original magnet	Anisotropic $B \parallel$ easy-axis	Bulk	1.39	1114	7.56

Table 1. Intrinsic remanence and coercivity determined from magnetization curves of recycled samples at $T = 20\text{ }^\circ\text{C}$ as shown in figure 5 and 6. The last column is showing the density of the samples.

References

- [1] M. Sagawa, S. Fujimura, H. Yamamoto, Y. Matsuura & K. Hiraga, “Permanent magnet materials based on the rare earth-iron-boron tetragonal compounds”, IEEE Trans. Magn. 20, 1584–1589 (1984)
- [2] K. Habib, P. K. Schibye, A.P. Vestbø, O. Dall & H. Wenzel, “Comprehensive Waste Flow Sampling and Analysis Approach”, Environ. Sci. Technol. 48, 12229–12237 (2014)
- [3] M. Zakotnik, I. R. Harris & A. J. Williams, “Multiple recycling of NdFeB-type sintered magnets”, J. Alloys Compd. 469, 314–321 (2009)
- [4] R. S. Sheridan, R. Sillitoe, M. Zakotnik, I. R. Harris & A. J. Williams, “Anisotropic powder from sintered NdFeB magnets by the HDDR processing route”, J. Magn. Magn. Mater. 324, 63–67 (2012)
- [5] W.F. Li, T. Ohkubo, K. Hono & M. Sagawa, “The origin of coercivity decrease in fine grained Nd-Fe-B sintered magnets”, J. Magn. Magn. Mater. 321, 1100–1105 (2009)
- [6] M. Sagawa, “NdFeB sintered magnet production method and production device and NdFeB sintered magnet produced with said method”, Patent WO 2011/024936 (2012)

- [7] K. Kobayashi, K. Urushibata, Y. Une and Masato Sagawa, “The origin of coercivity enhancement in newly prepared high coercivity Dy-free Nd-Fe-B sintered magnets”, *Journal of Applied Physics* 113, 163910 (2013)
- [8] Y. Yang, A. Walton, R. Sheridan, K. Güth, R. Gauß, O. Gutfleisch, M. Buchert B. Steenari, T. Van Gerven, P. T. Jones and K. Binnemans, “REE Recovery from End-of-Life NdFeB Permanent Magnet Scrap: A Critical Review”, *J. Sustain. Metall.*, DOI 10.1007/s40831-016-0090-4 (2016)
- [9] A. Aharoni, “Demagnetizing factors for rectangular ferromagnetic prisms”, *J. Appl. Phys.* 83(6), 3432–3434 (1998)
- [10] D. Eckert, P. Nothnagel, K.-H. Müller and A. Handstein, “The influence of texture on the magnetization behaviour of sintered Nd-Fe-B magnets”, *Journal of Magnetism and Magnetic Materials* 101, 385-386 (1991)
- [11] M. Zakotnik et al., “Possible methods of recycling NdFeB-type sintered magnets using the HD/degassing process”, *Journal of Alloys and Compounds* 450 (2008) 525–531
- [12] Y. Shinba, T. J. Konno, K. Ishikawa, and K. Hiraga and M. Sagawa, “Transmission electron microscopy study on Nd-rich phase and grain boundary structure of Nd–Fe–B sintered magnets”, *J. Appl. Phys.* 97, 053504 (2006)
- [13] I. R. Harris, P. J. McGuinness, D. G. R. Jones and J. S. Abell, “Nd-Fe-B Permanent Magnets: Hydrogen Absorption/Desorption Studies (HADS) on Nd₁₆Fe₇₆B₈ and Nd₂Fe₁₄B”, *Physica Scripta*. Vol. T19, 435-440 (1987)

Figure captions

Fig.1. Illustration of the Hydrogen Decrepitation Press-Less Process (HD-PLP) recycling of anisotropic sintered NdFeB magnet. Passivated commercial N48M sintered magnets were used as starting material and hydrogen was applied to disintegrate the magnets inside a ball milling container. The hydride powder was both used directly and some powder was further disintegrated by subsequent ball milling. Size fractions of 28, 50 and 100 μm were obtained by simple sieving of the powder. Different size fraction were filled into graphite crucibles and packed to a density of 3 g/cm^3 . The powder particles were aligned by an external magnetic field and sintered in a vacuum furnace. The samples were removed by flipping the crucibles, whereby the samples fell out due to the shrinkage during sintering.

Fig. 2. Scanning Electron Microscopy (SEM) image showing the microstructure of original passivated N48M magnet used as starting material for HD-PLP recycling.

Fig. 3. Scanning Electron Microscopy (SEM) images showing the microstructure of samples made from hydride powder sieved into size fractions and by HD-PLP sintering at $T = 1110\text{ }^{\circ}\text{C}$ for 2 hours: a) $d = 50\text{--}100\text{ }\mu\text{m}$, b) $d = 28\text{--}50\text{ }\mu\text{m}$ and c) $d < 28\text{ }\mu\text{m}$.

Fig. 4. Scanning Electron Microscopy (SEM) images showing the microstructure of samples made from hydride powder, which was ball milled in argon, sieved into size fractions and HD-PLP sintering at $T = 1110\text{ }^{\circ}\text{C}$ for 2 hours: a) $d = 50\text{-}100\text{ }\mu\text{m}$, b) $d = 28\text{-}50\text{ }\mu\text{m}$.

Fig.5. Magnetization curves of isotropic recycled magnets based on hydride powder sieved into size fractions (full line) and ball milled powder (dashed), as well as the initial N48M anisotropic magnet used as starting material (blue).

Fig.6. Second quadrant magnetization curve of anisotropic samples made from N48M hydride powder with $d < 100\text{ }\mu\text{m}$ and aligned in magnetic field of $B_a = 1.5\text{ T}$: Loose powder aligned perpendicular to crucible axis with no further packing (black), powder packed and then aligned parallel to crucible axis (green), powder packed and then aligned perpendicular to crucible axis (red) and the original N48M magnet (blue).

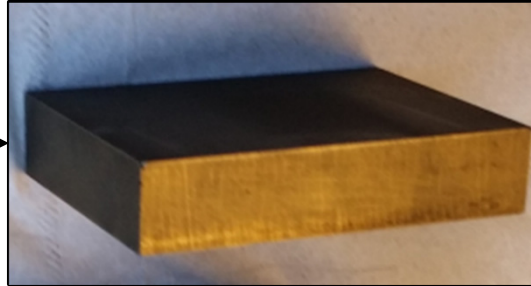
Fig.7. Magnetic phase diagram showing intrinsic remanence B_r and coercivity H_{ci} of isotropic ball milling powder recycled magnets (red), isotropic hydride powder recycled magnets (black) and the original anisotropic N48M magnet (blue). Thick lines represent samples with densities above 6.9 g/cm^3 . The arrows indicate the temperature history of the magnetization of the hydride samples with $d > 28\text{ }\mu\text{m}$ observed when first heating (arrow pointing right) and subsequently cooling (arrow pointing left).

Fig.8. Illustration of possible mechanism for densification during the Press-Less Process sintering. a) Arrangement of identical spherical powder particles in a simple cubic (SC) lattice as a suggestion to a representation of the initial packing apparent density of 3 g/cm^3 of the PLP sintering. b) The arrangement of a) can be densified by moving every second layer half a unit cell distance, whereby a body centered cubic (BCC) arrangement of the powder particles is obtained. The unit cell lattice parameter is termed a , the radius of the particles r and the spacing l_1 and l_2 are estimates of the pore size in the BCC arrangement. The inset is showing the simple cubic and the body centered particle arrangement in the graphite crucible.

End of Life Products



Passivated N48M
Magnet ($R_2Fe_{14}B$)



H_2 + Ball Mill



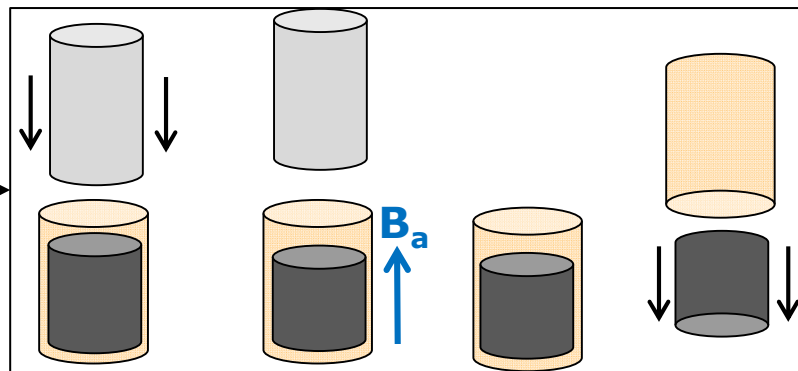
Sieve

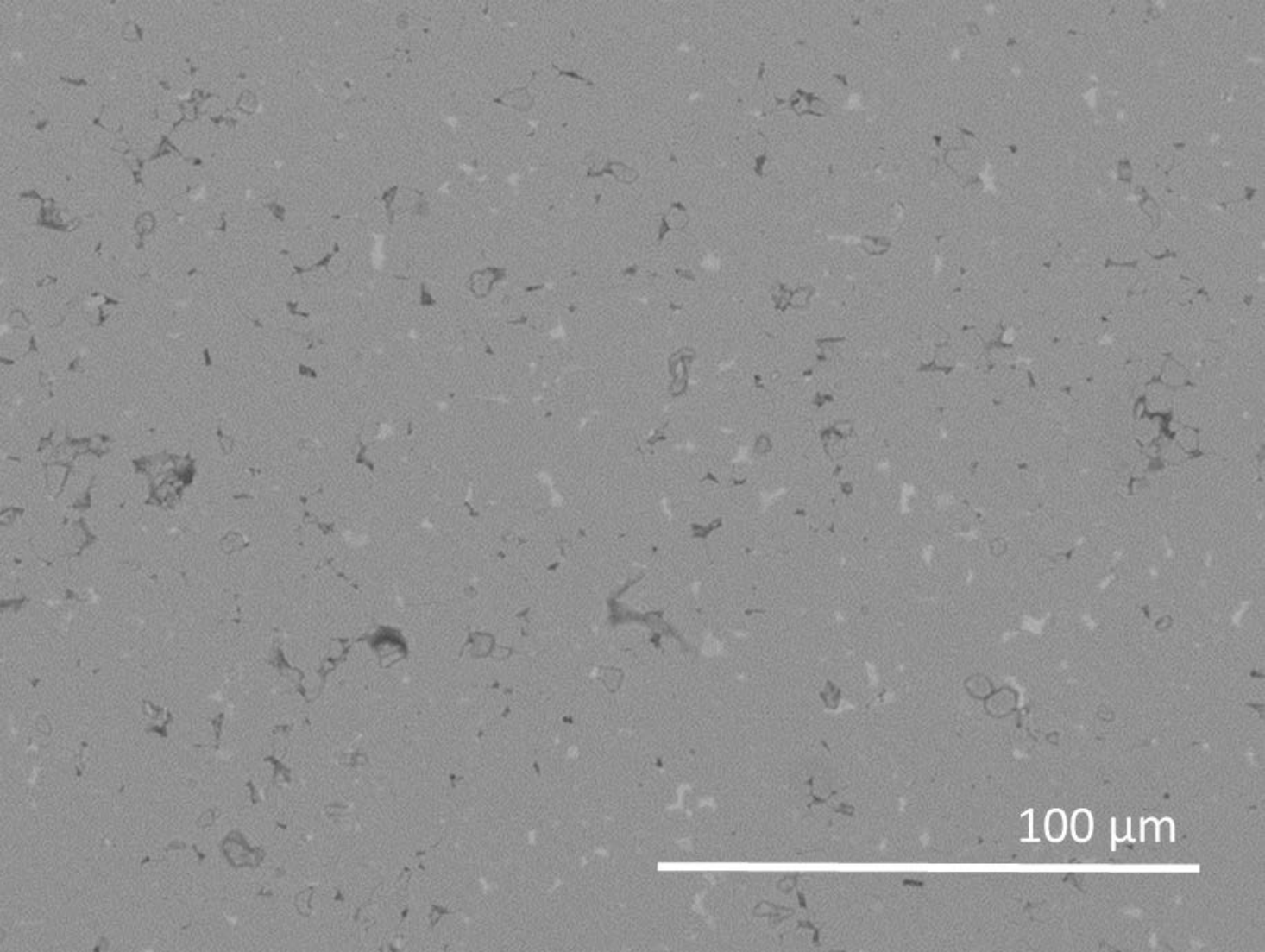


H_2 Decrepitated NdFeB Powder

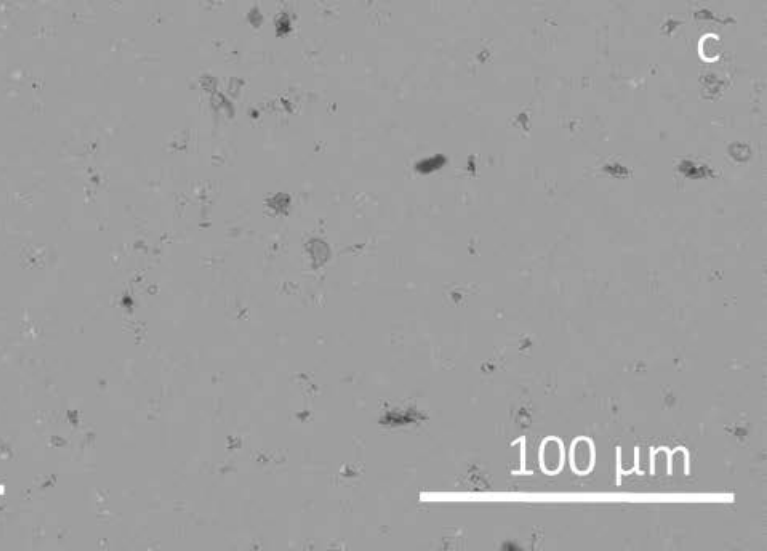
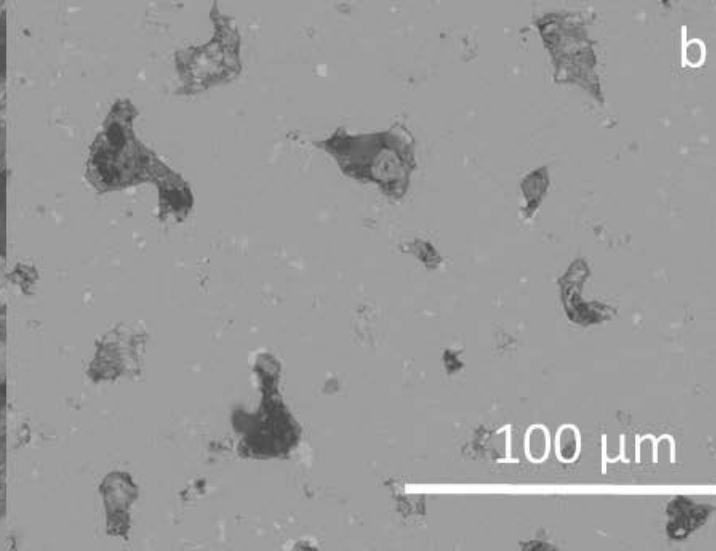
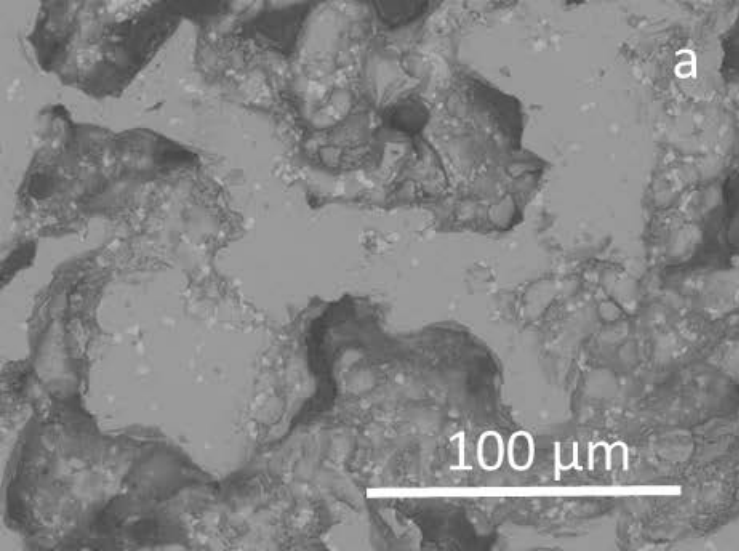


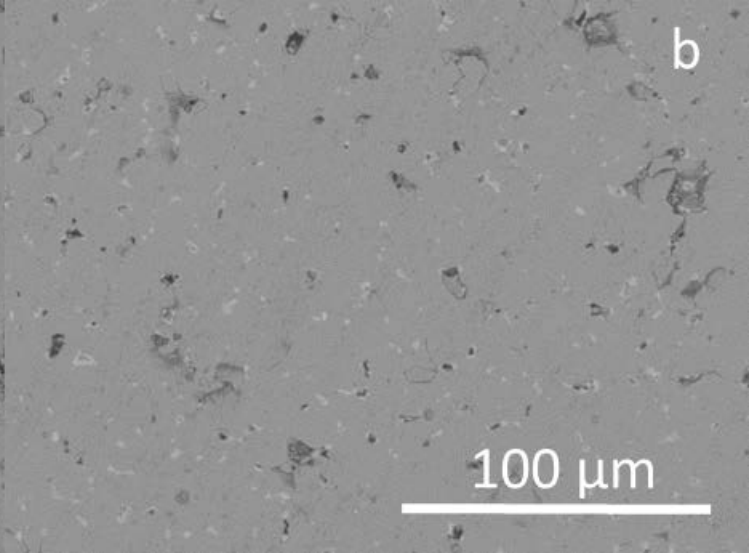
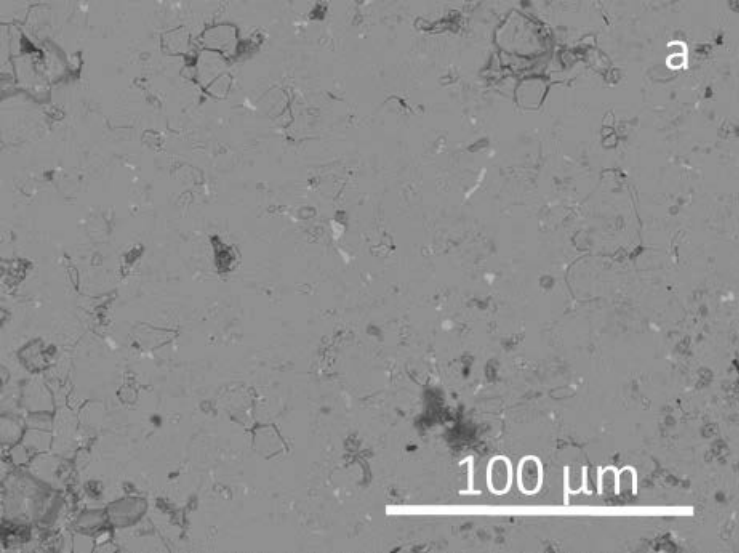
Sintering in Graphite Crucibles

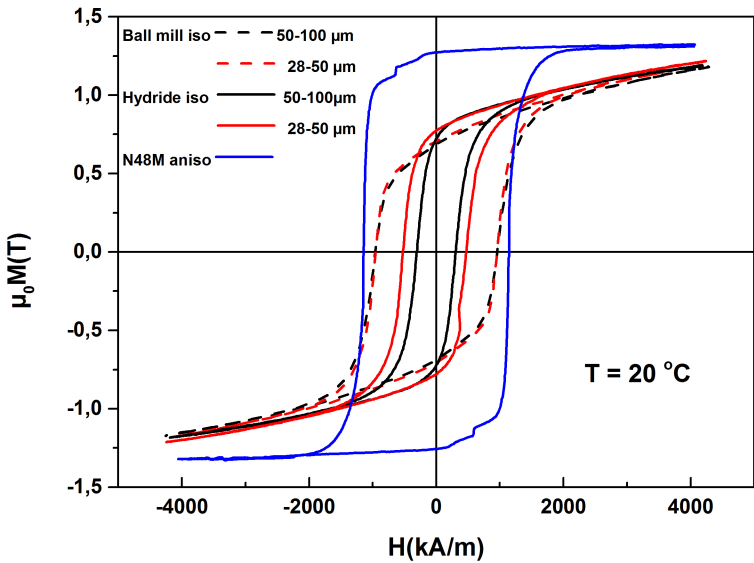


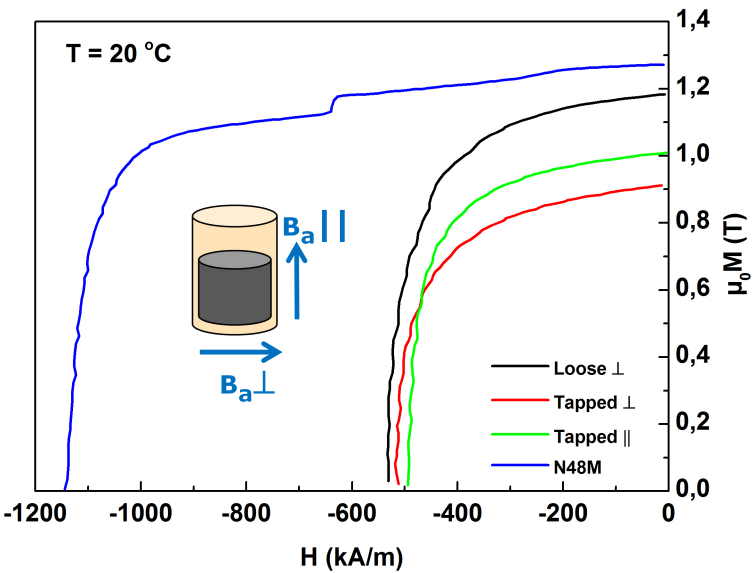


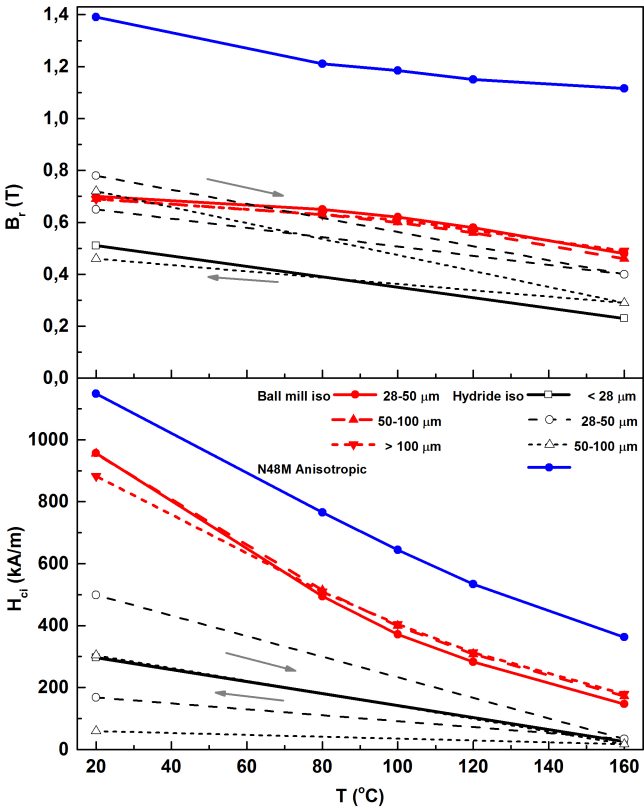
100 μm



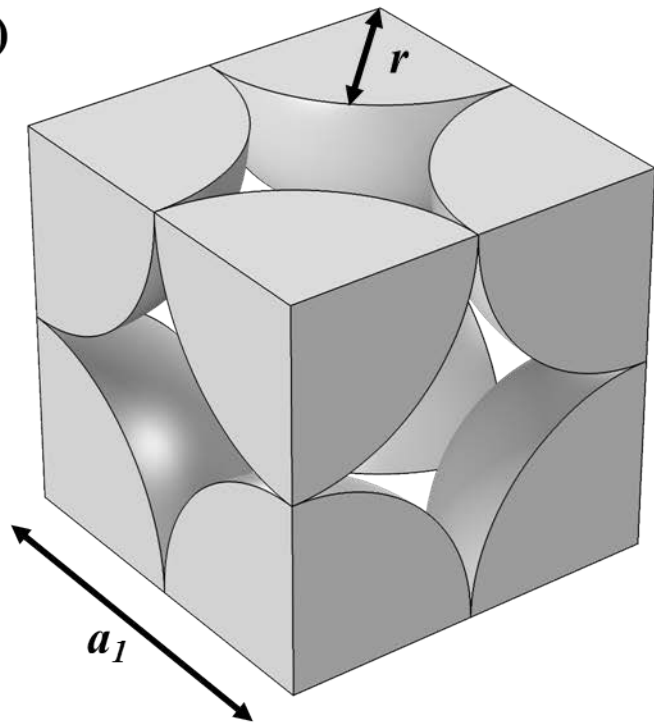




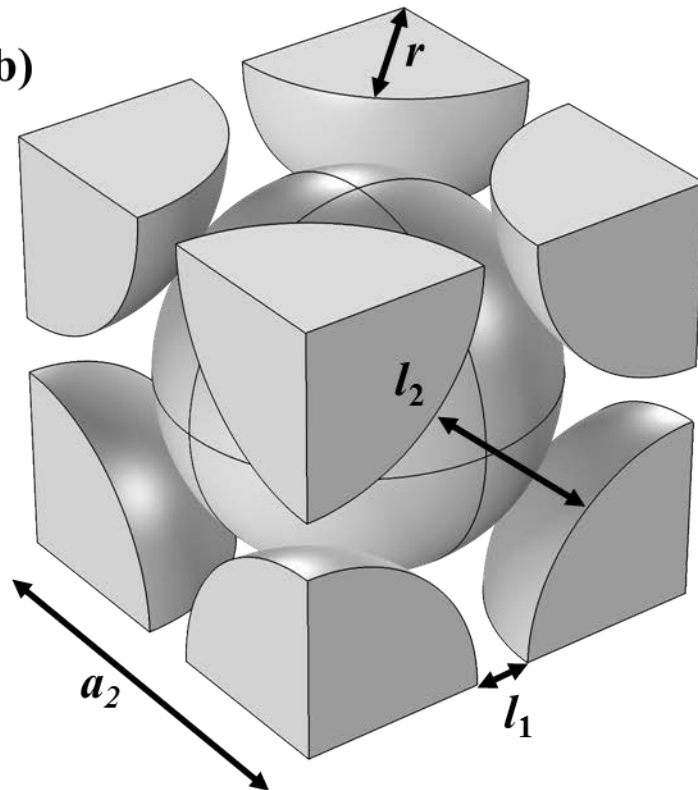




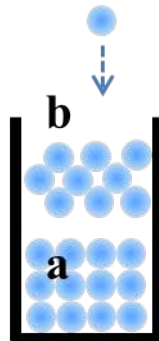
a)



b)



Powder particle



Graphite crucible